Proceedings World Geothermal Congress 2020+1
Reykjavik, Iceland, April - October 2021

Structural controls on fluid circulation in a transtensional duplex: Lessons from an exhumed geothermal system (Atacama Fault Zone, Chile)

Steven J Beynon, Daniel R Faulkner, David D McNamara, Rodrigo Gomila*, Erik Jensen**, Yan Lavallée

Department of Earth, Ocean and Ecological Sciences, University of Liverpool, UK

*Department of Geosciences, University of Padova, Italy
**Department of Geological Sciences, Universidad Católica del Norte, Antofagasta, Chile

steven.beynon@liverpool.ac.uk

Keywords: vein, fault, fluid flow, mineralisation, fracture sealing, quartz, calcite, epidote, fieldwork, duplex

Abstract

Geothermal reservoirs require high permeability to sustain fluid flow, which is often controlled by fracture networks. Mineral precipitation in veins within these fractures records interaction between fluids and deforming crust. Understanding vein formation processes in an exhumed geothermal system is fundamental to understanding fluid flow and efficiently exploiting modern geothermal systems in similar tectonic settings. The Caleta-Coloso transtensional duplex, part of the Atacama Fault Zone in Chile, is an analogue structural setting for a large proportion of geothermal systems. The duplex, formed almost entirely in granodirotic host rock, is bounded by two sinistral NNW-SSE strike-slip faults, and contains later ~NW-SE and ~E-W transtensional to extensional faults. Fractures in the fault damage zones contain a mineral assemblage of chlorite-epidote-quartz-calcite, recording a cooling geothermal system. Through analysis of mechanical damage and mineralogical data collected via linear transects and outcrop surface mapping, we characterize structural controls on episodic flow to help identify where may be most prospective in terms of permeability and fluid flux. Measurements of vein intensity suggest that areas within the duplex have undergone more brittle deformation than areas outside, with greater connectivity also suggesting higher paleo-permeability. There is a large degree of variability, however, with greatest paleo-permeability in a localised dilational jog near a major bounding fault, where each successive vein phase has exploited existing structures (crack-seal) but also creates linkage structures. Successive precipitation phases (i.e. fluid flow events) often form in different parts of the damage zone, suggesting earlier phases have significantly reduced permeability and/or increased rock strength. Vein thickness is used as a proxy for fluid flux, indicating the amount of sealing by precipitate. Nearest the bounding faults, high total thicknesses of all vein phases, alongside evidence of hydrobrecciation and crack-seal structures associates with epidote-bearing phases, suggest that ongoing high-temperature, high-pressure hydrothermal fluid flux has occurred consistently and over long timescales in these areas. In the duplex centre (dominated by few, thick, single-phase calcite veins), sporadic low-temperature high-flux fluids capable of propping open fractures succeeded short-lived, low-flux, higher-temperature fluid flow. Outside of the duplex it appears that fewer, less connected fracture orientations remained open, but potentially for longer periods. Ongoing related work aims to further consider vein microstructure to quantify mineral precipitation rates and pressure/temperature conditions to help constrain the longevity of these geothermal systems.

1. INTRODUCTION

1.1 Mineral Veins in Geothermal Systems

The Chilean Andes host one of the largest undeveloped geothermal provinces of the world. Chile currently imports nearly 85% of fossil fuels for electricity production and more than 75% of all its energy requirements (Lahsen et al., 2015). More than 300 geothermal areas are associated with recent or active volcanism; these potential resources could provide a significant renewable energy source. Natural and enhanced geothermal resources are increasingly found to be hosted in low primary permeability crystalline reservoirs, within which fluid flow is largely controlled by faults and fracture networks (Bertani, 2015; Brace, 1980; Dezayes et al., 2010). Geothermal reservoirs require high permeability and near-hydrostatically pressured fluids (i.e. high flow rates) to efficiently transport hot fluids to the surface (Limberger et al., 2018; Sibson, 2000). The field study of fracture networks in exhumed epithermal systems offers greater insight into fracture-forming processes than drilling and geophysical studies alone (Hedenquist & Lowenstern, 1994), especially where no surface manifestations are evident. This is particularly true in favourable tectonic settings such as extensional duplexes (i.e. releasing bend stepovers or dilatational jogs). Such structures develop as a fault periodically propagates on one side of the structure and ‘shuts off’ the fault on the other side (Cembrano et al., 2005; Christie-Blick & Biddle, 1985; Cunningham & Mann, 2007) (Figure 1d), and comprise extensional-shear and purely extensional vein-fractures (Sibson, 1996). Around one third of systems in the Great Basin (USA) are hosted in such complex tectonic settings; other examples include the Coso field, California (Lees, 2002) and the Cerro Prieto field, Mexico (Glowacka et al., 1999). Fluid pathways are kept open long-term as networks of critically stressed, closely spaced fractures (Faulds et al., 2011, 2013). Complex structures may however also inhibit fracturing and fluid flow (Cunningham & Mann, 2007). This study aims to explore the fluid flow history of the Caleta Coloso duplex, part of the Atacama Fault Zone in northern Chile, using structural and compositional analyses of mineral veins to help identify where within a transtensional duplex may be most prospective in terms of permeability and fluid flux.

In low porosity rocks, the cores of upper crustal faults typically comprise low permeability fault gouge and cataclasites, adjacent to a more permeable fractured damage zone (Faulkner et al., 2010, 2011; Faulkner & Rutter, 2000). Preferential fluid flow in the damage zone promotes vein formation, with factors such as palaeostress orientations, physio-chemical mineral growth, reseal hardening/weakening and crack-seal mechanisms playing an important role (Bons et al., 2012; Faulkner & Armitage, 2013; Ramsay, 1980; Sibson, 1996; Woodcock et al., 2007). At the matrix scale, structural permeability is controlled by the interplay of microstructural characteristics, such as fracture length, aperture and density (Mitchell & Faulkner, 2008). In order to understand the evolution of geothermal systems and develop them successfully, it is important to study how fracture networks form (i.e. stress and reservoir mechanics (Davatzes & Hickman, 2010)), how they may seal with minerals precipitated from geothermal fluids (Dobson

et al., 2003), and their crack-seal cycle history (McNamara et al., 2016). The same fractures that operate as interconnected, open fluid pathways can also behave as fluid barriers as they are continuously sealed by hydrothermal mineralization (Bons et al., 2012), decreasing permeability and the efficiency of a potential resource (Dobson et al., 2003). Pressure and temperature fluctuations may then reverse these reactions, causing mineral break down that result in porosity and permeability generation (e.g., Heap et al., 2012, 2013). The mineralogy, geochemistry and microstructure of mineral veins provides a record of pressure, temperature and strain history, fluid compositions, and interactions between fluids and fractured host rock (Bons et al., 2012). Study of how hydrothermal veins may seal and influence palaeo-permeability in fossil hydrothermal settings is critical to establishing the evolution and sustainability of fractured geothermal systems (Gomila et al., 2016; Sibson, 1996). The episodic spatial and temporal relationship between fluid flow, fracturing and fracture healing and how this changes with distance from the fault core in structurally anisotropic and discontinuous brittle fault zones is not well understood (Gomila et al., 2012), yet this can aid in the overall understanding of mechanical and hydraulic reservoir properties relevant to geothermal exploration.

1.2 Structural Overview of the Caleta Coloso Duplex

The Atacama Fault Zone in northern Chile (Figure 1a,b) developed as a sinistral arc-related fault between 190-110Ma, owing to oblique SE subduction of the Aluk plate beneath South America (Cembrano et al., 2005; Scheuber & Andriessen, 1990; Scheuber & González, 1999). Individual ductile dip-slip events have been dated using fission track analyses at ~145Ma, and later brittle strike-slip events at ~125Ma (Scheuber & Andriessen, 1990; Scheuber & González, 1999). Miocene-Pliocene normal dip-slip reactivation has also been documented and attributed to the ENE-subduction of the Nazca plate (González et al., 2006). Host rock in the field area comprises Early Jurassic ortho-amphibolite and ortho-granulite (Figure 1c) (Cembrano et al., 2005) intruded by late Jurassic diorite and granodiorite. NW-striking microdioritic dykes cut the igneous complex and represent the last igneous activity in the area (Cembrano et al., 2005). Both intrusion events induced mylonitic foliations, as evidenced by layers of annealed amphibole and plagioclase associated with NE-striking shear zones (Scheuber & González, 1999).

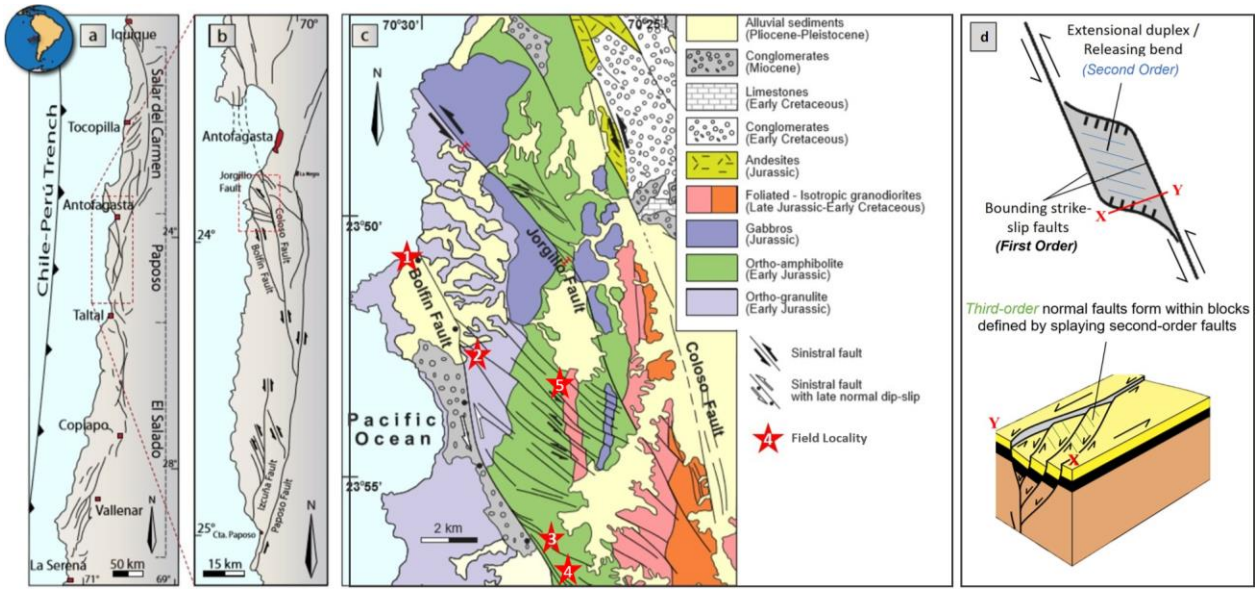

Figure 1: a) & b) Simplified structural map of the Atacama Fault Zone and c) Simplified geological map of the field area (modified from Cembrano et al., 2005). Field localities (described in Section 2.1) are marked as red stars. d) Simplified schematic diagrams of an extensional duplex between two sinistral strike-slip faults (in plan view, as well as cross sectional view across the transect X-Y) (adapted from Wakabayashi et al., 2004 and Cembrano et al., 2005).

The Caleta Coloso duplex is bounded by two overstepping NNW-trending master strike-slip faults (the Boflin and Jorgillo Faults) (Figure 1c,d), which are connected by a set of ~NW-SE-trending second-order transtensional faults dipping steeply to the NW. Sinistral movement on the faults is, at a minimum, ~10-200m (Cembrano et al., 2005). ~E-W-trending third-order extensional faults later formed within blocks defined by the second-order faults (Figure 1d), with growth mineral fibres and Riedel shears indicating normal displacement of up to ~10cm (Cembrano et al., 2005). These often form a mini duplex between second order faults and are dominant at outcrop scale. Stretching with a N-S orientation within the duplex may have been accomplished via progressive sinistral/normal displacement on master faults, leading to clockwise rotation of the inner blocks.

The hanging wall of the Bolin Fault, forming the western boundary of the duplex, is more deformed than the footwall, and comprises metre-wide cataclasites either side of cm-wide gouge. Duplex imbricate faults (i.e. 2nd and 3rd order faults) host mineralised veins and faults, whereas master faults are mainly sites of shear displacement (Cembrano et al., 2005), as predicted by the suction pump mechanism (Sibson, 1990) for transtensional duplexes. Chlorite-epidote-quartz-calcite shear and extension veins have been identified within the damage zones of faults within the duplex (Herrera et al., 2005), suggesting a strong link between fluid transport, mineral precipitation and brittle duplex development under low greenschist facies conditions (Cembrano et al., 2005). Hydrothermal veins likely formed contemporaneously with duplex development (Scheuber & Andriessen, 1990) prior to being passively exhumed, preserving structures representative of those formed at >3km depth (Cembrano et al., 2005).

2. METHODOLOGY

Fieldwork was carried out over two field seasons in 2019 and 2020, with several well-exposed field areas (Figure 1c) identified based on satellite mapping and previous field campaigns. The most common technique used to sample vein or fracture networks in the field - and the method used in this study - is via a linear scanline (1D transect), where the orientation, frequency, spacing and

thickness (aperture) of each vein intersected by the line is recorded (Ortega et al., 2006; Priest, 1993; Sanderson & Nixon, 2015) (Figure 2). 2D analyses were also made by digitally tracing fractures in orthomosaics captured via a drone-mounted camera, and selected outcrops were analysed using FracPaQ (Healy et al., 2017). Oriented samples were also taken systematically at each locality to further investigate vein microstructures.

Locality 1 is a coastal outcrop of the hanging wall ~280m west of the Bolfin Fault core, where one 1D structural transect and one 2D map was made. Locality 2 is an ~E-W trending gully, ~180m East of the Bolfin Fault, cutting a second-order fault of the Bolfin at the northern mapped limit of the duplex, where three 1D structural transects were made. Further south at Locality 3, steep ~NE-SW trending gully with good sub-horizontal and sub-vertical exposures transects a dilational jog, ~200-370m East of the Bolfin Fault, where three 1D transects and one 2D map were made. Locality 4 (described by Jensen et al., 2011) is a distributed second order splay of the Bolfin Fault outcropping in a wide NNE-SSW trending gully ~200 m East of the main fault, where three 1D structural transects and one 2D map were made. Locality 5 (described by Arancibia et al., 2015) comprises ~E-W gullies with both sub-vertical and sub-horizontal outcrops, situated ~3000m East of the main Bolfin Fault, and ~1950m West of the Jorgillo Fault, where three 1D structural transects were made.

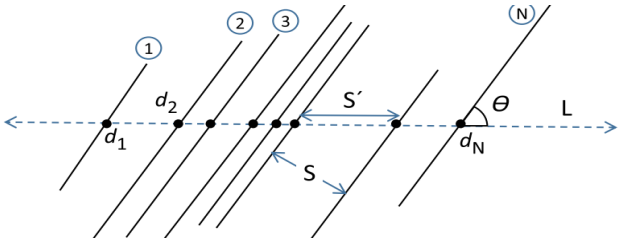

Figure 2: A linear scanline encountering N fractures over length L. Each fracture is a distance d from a reference point and oriented at an angle θ to the scanline. Spacing S' between each fracture is measured perpendicular to the scanline (but can also be measured perpendicular to the fracture (S)). (Modified from Sanderson & Nixon, 2015).

In this study, 1D data were analysed for a) all veins and b) individual vein phases at both transect and site level. Actual and cumulative vein frequency (N), vein spacing (S') and vein thickness (T) with distance (d) from the fault along were measured along line L (Figure 2). From this, normalised average intensity (P_{10}) was also calculated (N/L), which is an important attribute in assessing the fluid flow properties of a rock mass. Within a 2D area (A), P_{21} was also be calculated as N/A, providing additional insight into how veins and fractures interact (Sanderson & Nixon, 2015). To be comparable at site level, data from individual transects were normalised for transect length, and only sites a similar distance from a second-order fault (where known) were directly compared. Topology of vein networks was analysed in terms of the relative proportions of connecting nodes (terminations), which may be isolated (I), abutting (Y) or crossing (X) (Sanderson and Nixon, 2015). These proportions reflect the connectivity between veins, with a greater number of Y+X nodes typically resulting in higher palaeo-permeability (Healy et al., 2017).

3. RESULTS AND DISCUSSION

3.1 Spatial Distribution of Structures

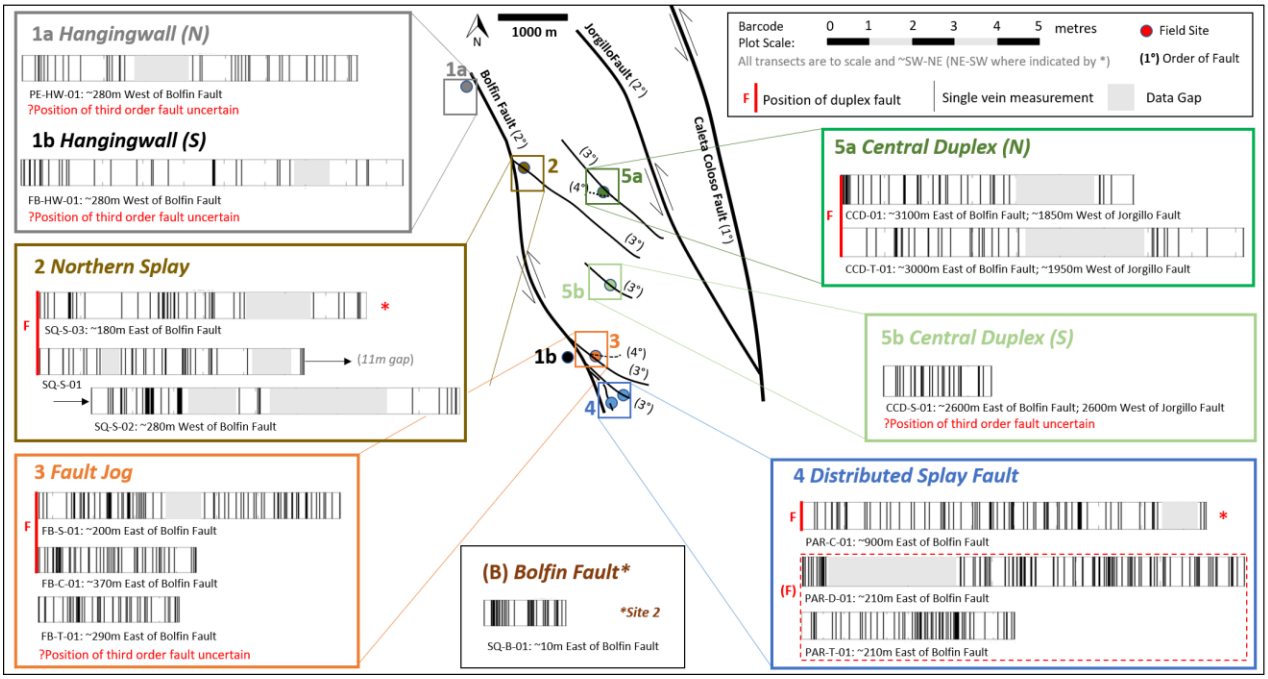

Figure 3: Stick plots for each 1D transect taken across the Caleta-Coloso Duplex, grouped by site (1= Hangingwall, 2 = Northern Splay, 3 = Fault Jog, 4 = Distributed Splay Fault, 5 = Central Duplex). Each line represents a single recorded vein. Grey areas represent limited exposure at the outcrop. All transects are to scale and are displayed from SW to NE, except where marked by *, where transects are displayed from SE to NW. Red lines indicate their position with respect to a known third-order fault

Stick plots (Figure 3) displaying the location of intersection of each vein with the transect line provide a visual representation of vein distributions for each transect. Veining appears to be clustered throughout, and most intense near major 2nd order faults within the duplex than elsewhere in the fault zone. This is supported by higher average cumulative frequency:distance gradients (locality 3 = 14.8; 4 = 12.6) with respect to outside of the duplex (locality 1 = 4.07). Sites 2 and 5 (also within the duplex but near 2nd & 3rd order faults of apparently less displacement) have average gradients of 7.3 and 8.6 respectively. For comparison, immediately adjacent to the duplex bounding (1st order) Bolfin Fault the gradient of cumulative vein frequency is much higher at 29.9.

Average normalised vein intensity (P_{10}) (Figure 4a) in the hangingwall outside of the duplex (locality 1) is low (5.01±1.15 m^{-1}), with small standard deviations both within and between transects. Within the duplex, greatest P_{10} values are recorded at a fault jog near a major fault (locality 3 = 12.97±0.97 m^{-1}) and a distributed fault zone near a major fault (locality 4 = 12.40±2.31 m^{-1}). Vein intensity is somewhat lower at the edge of the duplex (locality 2 = 9.23±1.26 m^{-1}) and with greater distance from bounding faults (locality 5a = 7.90±1.10 m^{-1}). Also shown for comparison in Figure 4 is the vein intensity adjacent to the major duplex bounding fault (~23.50 m^{-1}). Standard deviations on these data indicate significant variability in P_{10} within transects inside the duplex (±2.9 – 3.9 m^{-1}), particularly at Site 4 (±4.6 m^{-1}), where high variability also occurs between transects.

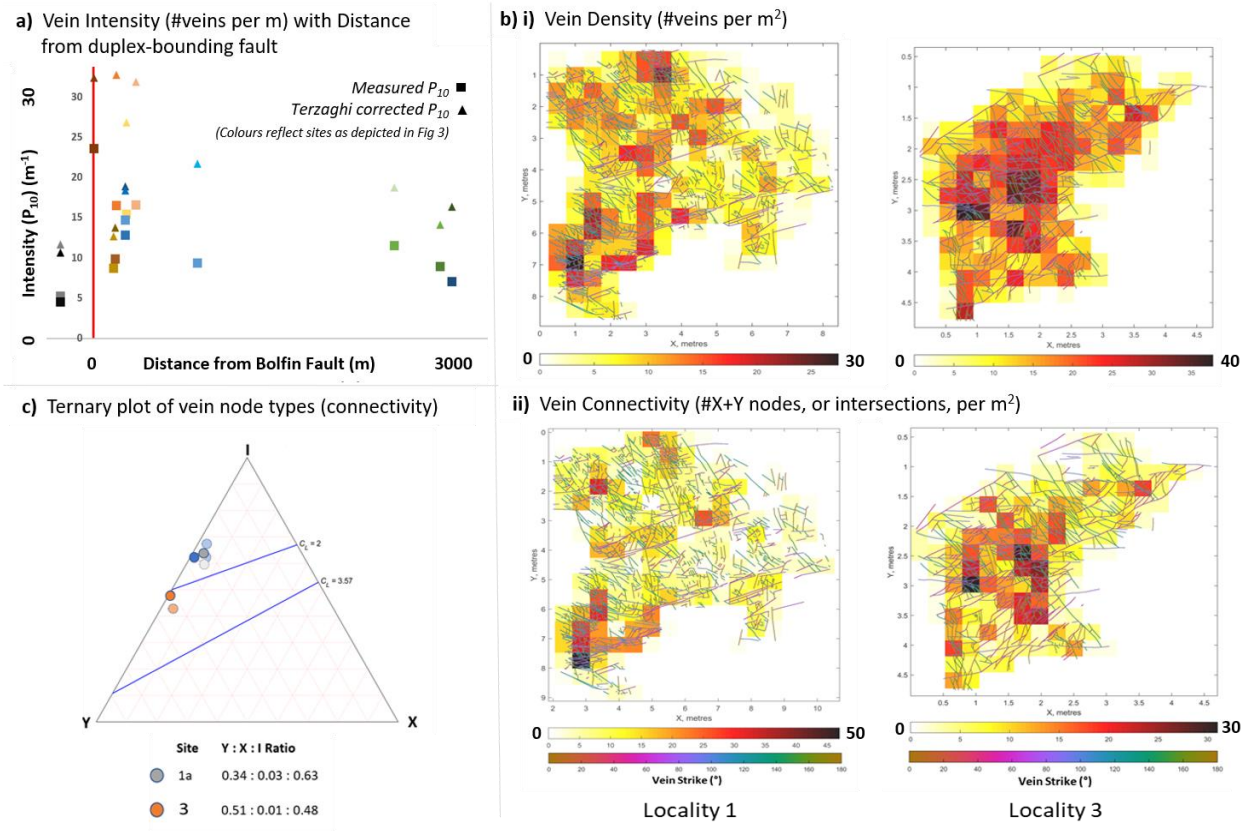

Figure 4: a) Average vein intensity (P_{10}, m^{-1}) with distance from the Bolfin Fault (0m, red); squares display measured data, and triangles display Terzaghi (1965) corrected data. All data are normalized for transect length with data gaps omitted. b) Maps of i) 2D vein density (P_{21}) and ii) vein connectivity from Site 1a, outside of the duplex and Site 3, within a dilational jog inside the duplex. c) Relative proportions of vein node types at localities 1 & 3 (I = isolated, Y = abutting, X = crossing). Maps generated using FracPaQ, overprinted on vein traces coloured by strike orientation.

Figure 4b(i) shows 2D variability in vein density (P_{21}) within and between sites. Average P_{21} is greatest at a fault jog near a major fault (locality 3 = 9.3 m^{-1}; max. 28.4 m^{-1}). Outside of the duplex, P_{21} is considerably lower (site 1a = 5.6 m^{-1}; max. 27.5 m^{-1}). Standard deviations indicate considerable variation at both sites. When compared to intensity data from 1D transects from the same outcrop (Figure 4a), locality 1 falls within the standard deviation, however 1D transects at locality 3 overestimates intensity by a factor of 3. Vein connectivity is estimated using the relative proportions of isolated (I) and connecting (X+Y) nodes. Figure 4b(ii) shows the distribution of connecting node density: Connectivity is greatest at locality 3, where the total ratio of (X+Y) to I nodes is 0.52:0.48, in comparison to 0.37:0.63 at locality 1 (Figure 4c). Within the duplex, connecting nodes are well-distributed throughout the outcrop, whereas outside of the duplex connecting nodes form clusters that partially coincide with clusters of vein density.

3.2 Spatial Distribution of Precipitate

Structural datasets have been analysed further in order to determine how vein thickness and composition changes in relation to position within the duplex (Figure 5), orientation (Figure 6) and distance from a fault core (Figure 7). Six precipitation types were identified in the field based on compositions and cross-cutting relationships: chlorite, chlorite+epidote (undifferentiated), epidote, epidote+quartz (undifferentiated), quartz, 'D3' (clay, salt and calcite), and calcite. These have been grouped into three broad vein phases: phase 1 (epidote-dominated) and 2 (quartz-dominated) often form a broadly coeval set with orientations relating to stress conditions imposed by 1st and 2nd order faulting (Figure 6). Crack-seal and shear microstructures are common (e.g. Figure 8). Veins formed during phase 3 (calcite-bearing) often exploit veins relating to 2nd order faults, however often form veins at orientations relating to 3rd order faults (Figure 6). Further analysis of vein orientation and vein textures is still ongoing.

Vein thickness, when calculated as a 1m-binned normalised average for each locality, is greatest at locality 5 (the centre of the duplex, at greatest distance from bounding faults) (4.22 mm) but shows considerable variability both between and within (±1.22 to 2.20 mm) transects. This is represented by a large value for total measured vein thickness in Figure 5. Other localities within the duplex (2 to 4), show smaller average thicknesses (2.40 - 3.03 mm), with generally lower standard deviation, particularly at locality 3 (±0.17 to ±1.49mm), indicating more regional consistency. Minimum values for total amount of precipitate per unit length are outside of the duplex (locality 1) (Figure 5). Precipitation across the duplex is dominated by epidote-bearing phases (green/blue-green in Figure 5), particularly within the fault jog adjacent to a major fault (locality 3). Locality 5 is anomalous in that a small number of thick calcite veins and thick quartz veins dominate the total amount of precipitate.

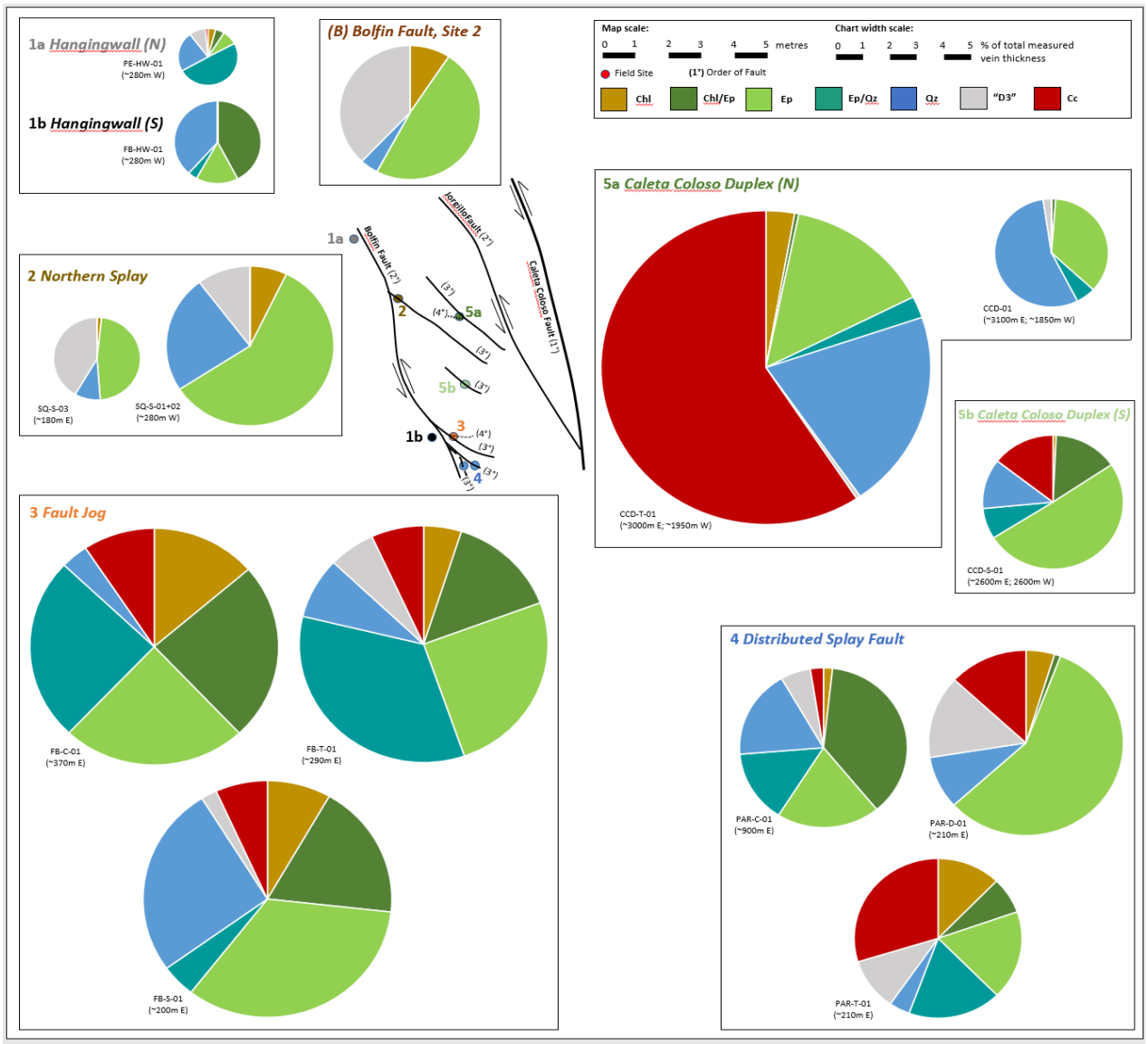

Figure 5: a) Total cumulative thickness proportions of six vein phases at five localities within the duplex (see main text for details). The size of each pie represents the total amount of precipitate (% of total measured vein thickness) in each 1D transect.

Analysis of vein orientations is in early stages, however preliminary results (Figure 6) highlight considerable differences in the complexity of the fracture-hosted vein network outside and within the duplex. Outside of the duplex (locality 1), all epidote- and quartz-bearing veins appear to be perpendicular to 1st order duplex-bounding faults or roughly parallel to a 2nd order fault, suggesting exploitation of existing structural features rather than creation of new ones, and there is little late-stage precipitation (Figure 5). Within the duplex (locality 3), the picture is complicated by the fact that 1st, 2nd and 3rd order faults interact and apparently overlap both spatially and temporally; almost every vein phase (representing the long-term assemblage) is shown to exploit structures relating to every fault order. Field observations suggest that within the duplex new fractures are created as well as existing veins being exploited.

Initial analysis of volume of precipitate (an extrapolation of binned vein thicknesses) with distance from a 2nd order fault at locality 2 (Figure 7) suggests that the precipitate volume of phase 1 & 2 veins (which in general follow a similar trend to the 2nd order fault) is much greater in the western footwall of the fault. Phase 3 veins are confined to the eastern hanging wall, ~2-5m from the fault core, and concentrated in a few major fractures ~4m east of the fault. Vein density in general also decreases with distance from the fault, particularly in the hanging wall. Preliminary XRF data suggests a depletion of Si and Al and enrichment of Fe and Mg nearest the fault (particularly to the west), potentially as a result of epidote-bearing vein distribution. Ca is depleted on the western side of the fault and near the fault on the eastern side, which may relate to the distribution of either epidote or calcite-bearing veins.

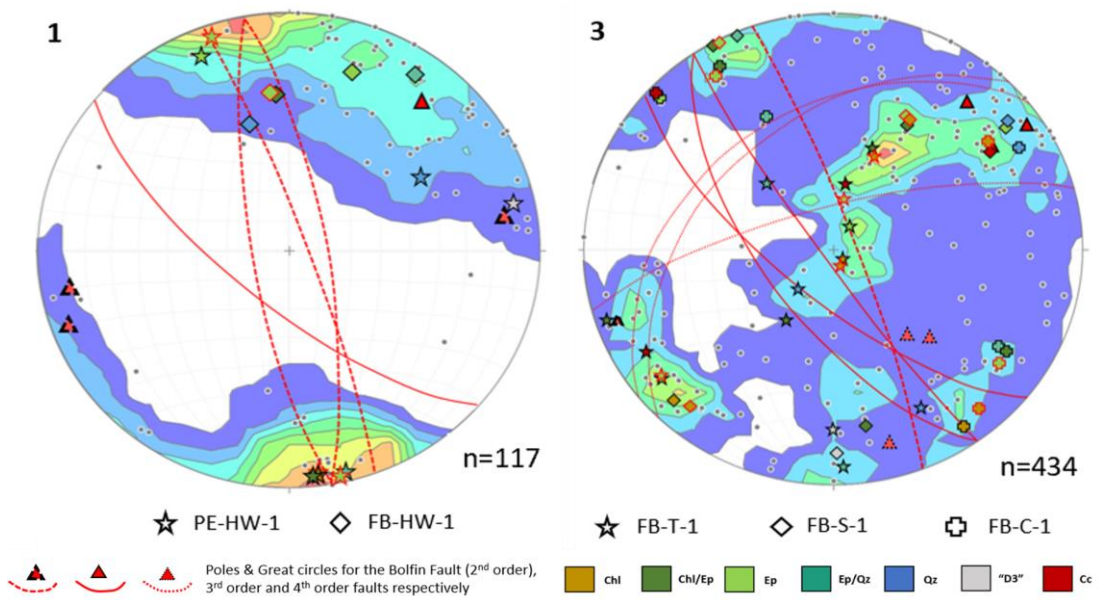

Figure 6: A comparison of average poles of each vein phase (with the Terzaghi (1965) correction applied) for each transect at localities 1 and 3. Kamb contours represent all veins measured at that locality.

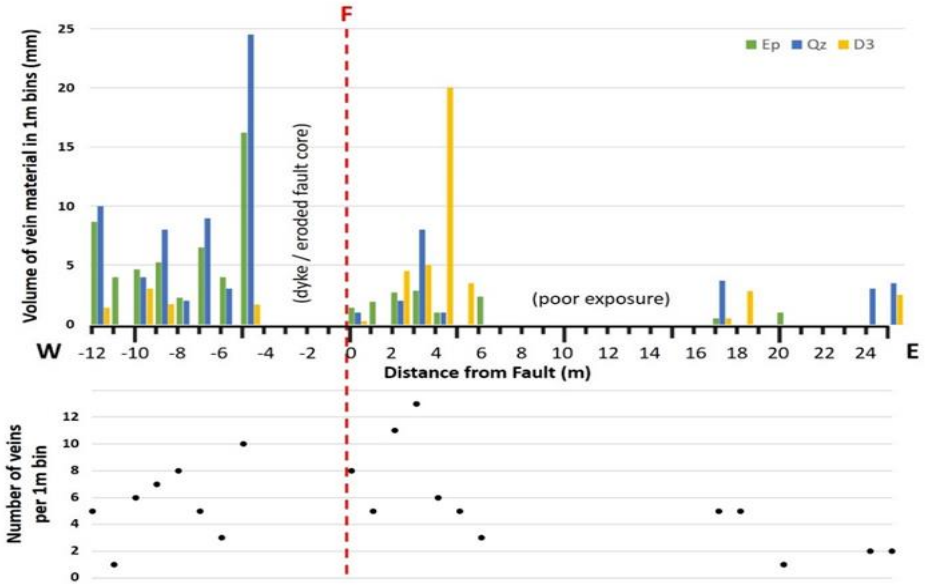

Figure 7: Change in precipitate volume (for epidote-dominated, quartz-dominated, and calcite-dominated (D3) veins) with distance from a 2nd order fault (F) at locality 2, normalized for number of veins (Scatter plot = vein density).

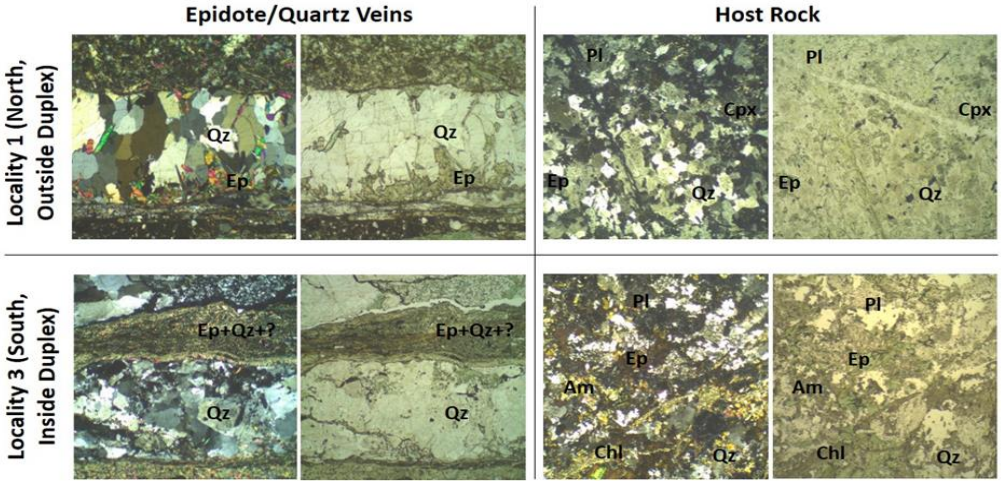

Figure 8: Photomicrographs of a phase 1 epidote-quartz vein and host rock from (top row) Locality 1 and (bottom row) Locality 3, Host rock images taken ~10mm from the vein wall. Qz = quartz, Ep = epidote, Pl = plagioclase feldspar, Am = amphibole, Cpx = Clinopyroxene, Chl = chlorite. All images at 2.5x magnification in xpl (left) and ppl (right).

Petrographic and geochemical analyses of host rock adjacent to veins (Figure 8) are in progress but aim to give an overview of the vein texture and degree of related host rock alteration and deformation. Outside of the duplex (locality 1), host rock is relatively fresh granodiorite comprising mostly undeformed plagioclase feldspar, quartz and clinopyroxene with minor (<10%) epidote. Phase 1 vein walls are typically well defined and planar, with euhedral epidote crystals elongated perpendicular to the quartz-dominated vein walls forming a syntaxial/epitaxial texture. Within the duplex (locality 3), host rock composition is that of an altered granulite, comprising deformed and party altered plagioclase feldspar, amphibole (hornblende) and quartz with a greater proportion of alteration products chlorite and epidote (~35%). A markedly different texture shows multiple quartz-rich and epidote-rich bands potentially representing crack-seal mechanisms. Quartz-rich bands contain fine- to medium-grained subhedral crystals in a blocky texture. Epidote-rich bands are very fine-grained and highly foliated.

4. DISCUSSION: SUMMARY AND POTENTIAL IMPLICATIONS

Whilst it must be noted that data shown here is preliminary and represents a small subset of all acquired field data, initial analyses of vein structural and compositional data from an exhumed transtensional duplex-hosted geothermal system highlight several implications for successful and sustainable exploitation of a contemporary system. This brief discussion will focus on inferred pressure/temperature conditions and spatial distribution of fluid flow (including exploitation of pre-existing structures).

In this exhumed extensional duplex-hosted geothermal system, we observe a propylitic mineral assemblage generally indicative of Fe- and Mg-bearing hydrothermal fluids causing alteration of amphiboles (Robb, 2004). Presence of chlorite and epidote is indicative of elevated temperatures (>260°C), whilst calcite is usually precipitated from fluids with high concentrations of dissolved CO_2 at temperatures of ~140–300°C (Simmons & Christenson, 1994). Mineral veins and their relationships to each other appear to record a long-lived but cooling geothermal system. Fluid inclusion data is currently being obtained for the veins sampled in this study, however Cembrano et al. (2005) suggest that veins in the study area formed at ~101-252°C. The dissolution and alteration of primary minerals, and precipitation of secondary minerals caused by the movement of hot, dissolved-ion rich fluids, affects the rock mechanical properties and distribution of permeable zones (e.g. Heap et al., 2012, 2013). Distributions of mineral phases around duplex faults here indicate that fractures exploited by late fluids are not the same as those exploited previously, suggesting that early precipitation has increased the strength of the rock mass and/or significantly decreased the permeability in some areas, such that calcite-precipitating fluids exploit the damage zone on the other side of the fault instead. This is likely to impact fluid pressures, the distribution of which strongly influences the style of faulting and mineralisation (Sibson, 1996). Observations at outcrop and in thin section within the duplex indicate widespread hydrothermal brecciation and crack-seal vein textures formed during the epidote-quartz deformation phase, which may be indicative of boiling, shear deformation or cyclic fracture collapse, or a combination of these processes. Crack-seal processes are generally associated with cyclic increases in fluid pressure and mineral stress concentrations (Wiltschko & Morse, 2001), but may also result from differential stress because of overlapping fault geometry (Cembrano et al., 2005). Veins outside of the duplex and at greatest distances from the bounding faults display markedly different structures indicative of less energetic formation processes (i.e. lower temperature and pressure) and less subsequent deformation.

The structural and compositional complexity of vein networks varies considerably regionally across the duplex, and often even at outcrop scale. This has implications for understanding the nature of fluid flow through these tectonic features and which areas may be considered suitable targets (or potential problem areas) for geothermal resource utilisation. All sites within the duplex tend to record intense, clustered vein networks (paleo-fluid flow zones), initially associated with the orientations of bounding faults, but later influenced more by 2nd- and 3rd-order faults. Fracture intensity and vein fill (a proxy for paleo-fluid flow) generally decreases with distance from both duplex-bounding faults and subsidiary faults as expected (Faulkner et al., 2010; McLean & McNamara, 2011; Schulz & Evans, 2000). Most intense mechanical damage and paleo-flow is apparent in areas adjacent to more major faults splaying from the duplex-bounding faults, with a range of compositions of high-temperature minerals suggesting overall long-term high-temperature fluid flux. In all areas except the central duplex, consistent vein thicknesses suggest consistent fluid flux, which is lower outside of the duplex. In the duplex centre, highly localised flow has precipitated fewer, wider, veins during later stages in the geothermal system, within which euhedral crystals appear to have grown into a cavity, possibly providing evidence of self-propping fractures allowing prolonged flow of fluids close to their supersaturation state (see Olivares et al., 2010; Beynon et al., 2021). Further analysis of vein microstructures will aim to develop this further, however extensional structures such as these could sustain high-flux, long-term fluid flow, relative to other individual shear/extensional structures that appear to be relatively short-lived and complex despite being situated in a more regionally-favourable area.

Whilst veins of particular orientations are repeatedly conducive to fluid flow across the duplex, additional structures at different orientations near bounding faults create linkage structures between them, as evidenced here via outcrop surface mapping showing greater vein connectivity within the duplex than outside. Anisotropy reactivation has important implications: preexisting structures appear to be important in controlling the onset of permeable fracture networks during later deformation and should be carefully considered when analysing a potential fractured geothermal reservoir. However, the orientation of structures with respect to the maximum principal stress (S_{Hmax}) is also important as it impacts which structures are critically stressed and thus potential fluid flow pathways (Sibson, 1996; 2000). Interactions with linking structures more representative of the regional stress creates connectivity that may produce a ~100-fold permeability increase (Kissling et al., 2015; Wallis et al., 2002). Mechanical anisotropy has most control on failure when the angle between the maximum principal stress (σ_1) and anisotropy is ~30° (Donath, 1961); structures of this orientation are more likely to open repeatedly and sustain long-term fluid flow, hence are also susceptible to more frequent crack-seal events (Davatzes & Hickman, 2010). Structures perpendicular to S_{Hmax} are most likely to open during relative extension, for example during periods of high fluid pressures under tensional local stress fields (Pérez-Flores et al., 2017; Sibson, 1996). Local cooling can also promote fracture opening via rock contraction (Lamur et al., 2018; Siratovich et al., 2015). Overall density and modes of vein orientations were observed to be greater within the duplex than outside, hence local stress concentrations within the duplex may be greater, promoting more frequent and widespread fluid flow that may be highly variable through individual structures. With current knowledge of the order of precipitation of the mineral assemblage coupled with understanding of stress in active extensional duplexes (Cunningham and Mann 2007; Sibson, 1996, 2000), we can infer that – at least in the dilational jog within the duplex – some, but not all, principal flow conduits and linkage structures would have been open to fluid flow at similar times. Outside of the duplex, less intense, more uniform vein distributions indicate overall lower fluid fluxes confined to structures of limited orientations, probably restricted to those containing pre-existing weaknesses.

5. CONCLUSIONS AND FURTHER WORK

Some preliminary data have been presented for a project that aims to understand the distribution and nature of mineral veins in an exhumed transtensional duplex, and how this affects the understanding of fracture-hosted fluid flow and permeability in structurally similar geothermal systems. The dataset highlights that pre-existing structures and location within a fault zone are critical factors to consider when assessing the suitability of a fractured geothermal reservoir, based on the following observations:

- Several vein-forming phases are observed to represent cooling fluid circulation within a complex, interconnected fracture network, preserved as an assemblage of chlorite-epidote-quartz-calcite-palygorskite-salt. Duplex veins commonly show coeval relationships, hydrothermal brecciation and crack-seal textures, suggesting episodic and energetic fluid flow.
- Indicators of mechanical damage around 2nd-order faults to a duplex-bounding fault, such as vein intensity (i.e. frequency & spacing) and connectivity, show that areas within an extensional duplex have experienced more deformation and fluid flux than areas outside of the duplex, inferred to represent higher palaeo-permeability. There is a large degree of variability in the amount of inferred fluid flow at a regional and outcrop scale, such that a dilational jog near a bounding fault has experienced most intense damage and fluid flux with little outcrop-scale variability. However, other areas within the duplex, particularly those away from major faults, show high outcrop-scale variability and generally less damage.
- Preexisting structures appear to be important in controlling the onset of permeable fracture networks during later deformation phases, acting as principal flow conduits. Within the duplex, particularly near bounding faults, additional complexity of linkage structures at orientations are important in increasing connectivity and permeability.
- Fracture density generally decreases with distance from faults, although veins (and hence principal fluid flow zones) within the duplex tend to form in clusters, compared to a more uniformly spaced distribution outside of the duplex. Successive precipitation phases form in different parts of the fault damage zone, suggesting early precipitation from fluid may significantly reduce permeability and/or increase rock strength.
- Sites adjacent to duplex bounding faults display relatively consistent vein thicknesses, representing the full range of compositions (i.e. pressure/temperature conditions) as well as plentiful evidence of host-rock alteration and crack-seal / hydrobrecciation structures. These are interpreted to signify long-term energetic fluid flux at high pressures and temperatures, although individual structures may not be open to flow for long. Vein thickness is most variable in the centre of the duplex, away from major faults, with the dominance of few, thick calcite veins suggesting sporadic but long-term high-flux events in individual pure-extension fractures in the later, cooler stages of the hydrothermal system.

As well as expanding the range of samples analysed in a similar approach to that outlined in this paper, particularly regarding vein thickness and orientation, future work aims to constrain the relative timings and formation conditions of vein microstructures and crystallographic precipitation phases, and as a result the evolving geothermal reservoir fluid properties and stress conditions. Several microscopy techniques (including cathodoluminescence, scanning electron microscopy) are to be applied to vein thin sections alongside fluid inclusion analysis. The combination of these techniques, supported by experimental rock deformation (Beynon et al., 2021), aims at establishing a better understanding of the physiochemical processes involved in mineral precipitation from geothermal fluids, including different crystal precipitation mechanisms and rates as a result of changing fluid compositions, pressures and temperatures.

ACKNOWLEDGEMENTS

Work presented here was conducted during a PhD study supported by the Natural Environment Research Council (NERC) EAO Doctoral Training Partnership, fully funded by NERC (Grant ref. no. NE/L002469/1), whose support is gratefully acknowledged. For their guidance, support and logistical assistance in the field, we would like to thank Giulio Di Toro, Giorgio Pennachioni, Michele Fondriest, Simone Masoch, Elena Spagnuolo and Giulia Magnarini. Thanks are also extended to Dave Healy & Roberto Rizzo for help with new scripts in FracPaQ.

REFERENCES

Bertani, R.: Geothermal Power Generation in the World 2010-2014 Update Report, *Proceedings: World Geothermal Congress, Melbourne, Australia*, (2015), 19–25.

Beynon, S. J., Faulkner, D. R., McNamara, D. D., and Lavalee, Y.: An Experimental Approach to Assist in Quantifying Fracture Sealing Mechanisms in Geothermal Systems, *Proceedings World Geothermal Congress, Reykjavik, Iceland*, (2021).

Boden, D. R: Geologic Fundamentals of Geothermal Energy, CRC Press (Editor: Ghassemi, A.), (2016), 423p.

Bons, P. D., Elburg, M. A., and Gomez-Rivas, E.: A Review of the Formation of Tectonic Veins and Their Microstructures, *Journal of Structural Geology*, **43**, (2012), 33–62.

Brace, W. F.: Permeability of Crystalline and Argillaceous Rocks, *International Journal of Rock Mechanics and Mining Sciences*, **17**, (1980), 241-251.

Cembrano, J., González, G., Arancibia, G., Ahumada, I., Olivares, V., and Herrera, V.: Fault Zone Development and Strain Partitioning in an Extensional Strike-Slip Duplex: A Case Study from the Mesozoic Atacama Fault System, Northern Chile, *Tectonophysics*, **400**(1–4), (2005), 105–125.

Christie-Blick, N., and Biddle, K. T.: Deformation and Basin Formation along Strike-Slip Faults, *In: Strike-Slip Deformation, Basin Formation and Sedimentation, SEPM Special Publication*, **37**, (1985) 1–34.

Cunningham, W. D., and Mann, P., Tectonics of strike-slip restraining and releasing bends, *Geological Society, London, Special Publications*, **290**, (2007), 1-12

Davatzes, N. C., and Hickman, S. H.: The Feedback Between Stress, Faulting, and Fluid Flow: Lessons from the Coso Geothermal Field, CA, USA, *Proceedings World Geothermal Congress*, *Bali, Indonesia*, (2010), 1–15.

Dezayes, C., Genter, A., and Valley, B.: Overview of the Fracture Network at Different Scales Within the Granite Reservoir of the EGS Soultz Site (Alsace, France), *Proceedings World Geothermal Congress, Bali, Indonesia*, (2010), 25–29.

Dobson, P. F., Kneafsey, T. J., Hulen, J., and Simmons, A.: Porosity, Permeability, and Fluid Flow in the Yellowstone Geothermal System, Wyoming, *Journal of Volcanology and Geothermal Research*, **123**, (2013) 313–324.

Donath, F. A.: Experimental Study of Shear Failure in Anisotropic Rocks, *Geological Society of America Bulletin*, **72**, (1961), 985–990.

Faulds, J. E., Hinz, N. H., Coolbaugh, M. F., Cashman, P. H., Kratt, C., Dering, G., et al.: Assessment of Favorable Structural Settings of Geothermal Systems in the Great Basin, Western USA, *Geothermal Resources Council Transactions*, **35**, (2011), 777–783.

Faulds, J. E., Hinz, N. H., Dering, G. M., and Siler, D. L.: The Hybrid Model - The Most Accommodating Structural Setting for Geothermal Power Generation in Great Basin, Western USA, *Geothermal Resources Council Transactions*, **37**, (2013) 4–10.

Faulkner, D. R., and Armitage, P. J.: The Effect of Tectonic Environment on Permeability Development Around Faults and in the Brittle Crust. *Earth and Planetary Science Letters*, **375**, (2013), 71–77.

Faulkner, D. R., and Rutter, E. H.: Comparisons of Water and Argon Permeability in Natural Clay-Bearing Fault Gouge Under High Pressure at 20°C, *Journal of Geophysical Research*, **105**(B7), (2000), 16415.

Faulkner, D. R., Jackson, C. A. L., Lunn, R. J., Schlische, R. W., Shipton, Z. K., Wibberley, C. A. J., and Withjack, M. O.: A Review of Recent Developments Concerning the Structure, Mechanics and Fluid Flow Properties of Fault Zones, *Journal of Structural Geology*, **32**(11), (2010), 1557–1575.

Faulkner, D. R., Mitchell, T. M., Jensen, E., and Cembrano, J.: Scaling of Fault Damage Zones with Displacement and the Implications for Fault Growth Processes, *Journal of Geophysical Research: Solid Earth*, **116**(5), (2011), 1–11.

Glowacka, E., Gonzalez, J., and Fabriol, H., Recent Vertical Deformation in Mexicali Valley and its Relationship with Tectonics, Seismicity, and the Exploitation of the Cerro Prieto Geothermal Field, Mexico, *Pure and Applied Geophysics* **156**(4), (1999), 591-614.

Gomila, R., Mitchell, T. M., Arancibia, G., Jensen, E., Rempe, M., Cembrano, J., Hoshino, K., and Faulkner, D. R.: Geochemistry and Fluid Inclusions Across a Crustal Strike-Slip Mesozoic Fault: Insights of Fluid-Flow / Rock Interaction in the Atacama Fault System, *AGU Fall Meeting Abstracts*, (2012), 2548.

Gomila, R., Arancibia, G., Mitchell, T. M., Cembrano, J. M., and Faulkner, D. R.: Palaeopermeability Structure Within Fault-Damage Zones: A Snap-Shot from Microfracture Analyses in a Strike-Slip System, *Journal of Structural Geology*, **83**, (2016), 103–120.

González, G., Dunai, T., Carrizo, D., and Allmendinger, R.: Young Displacements on the Atacama Fault System, Northern Chile from Field Observations and Cosmogenic 21Ne Concentrations, *Tectonics*, **25**(3), (2006), 1–15.

Heap, M. J., Lavallée Y., Laumann A., Hess K.-U., Meredith P. G., and Dingwell D. B.: How Tough is Tuff in the Event of Fire, *Geology*, **40**, (2012), 311-314.

Heap M. J., Mollo, S., Vinciguerra, S., Lavallée, Y., Hess, K.-U., Dingwell, D.B., Baud, P., and Iezzi G.: Thermal Weakening of the Carbonate Basement Under Mt. Etna Volcano (Italy): Implications for Volcano Instability, *Journal of Volcanology and Geothermal Research*, **250**, (2013), 42-60.

Healy, D., Rizzo, R. E., Cornwell, D. G., Farrell, N. J. C., Watkins, H., and Timms, N. E., FracPaQ: A MATLAB™ Toolbox for the Quantification of Fracture Patterns, *Journal of Structural Geology* 95, (2017), 1-16.

Hedenquist, J., and Lowenstern, J. B.: The Role of Magmas in the Formation of Hydrothermal Ore Deposits, *Nature*, **370**, (1994), 519–527.

Herrera, V., Cembrano, J., Arancibia, G., Kojima, S., and Prior, D.: Synkinematic Fluid Flow and Vein Formation by Depressurization in Magmatic Arcs: A Case Study from Atacama Fault System, northern Chile, *Society*, (2005), 372–375.

Kissling, W. M., Ellis, S., and McNamara, D. D.: Modelling Fluid Flow Through Fractured Rock: Examples Using TVZ Geothermal Reservoirs, *Proceedings: 37th New Zealand Geothermal Workshop*, (2015), 1–10.

Lahsen, A., Rojas, J., Morata, D., and Aravena, D.: Geothermal Exploration in Chile: Country Update, *Proceedings: World Geothermal Congress 2015, Melbourne, Australia*, (2015), 1-7.

Lamur, A., Lavallée, Y., Iddon, F., Hornby, A. J., Kendrick, J. E., von Aulock, F. W., and Wadsworth, F. B.,: Disclosing the Temperature of Columnar Jointing and Fluid Flow in Lavas, *Nature Communications*, **9**, (2018), 1432.

Lees, J. M., Three-Dimensional Anatomy of a Geothermal Field, Coso, Southeast-Central California, *Geological Society of America Memoir*, **195**, (2002), 259-276.

Limberger, J., Boxem, T., Pluymaekers, M., Bruhn, D., Manzella, A., and Calcagno, P.: Geothermal Energy in Deep Aquifers: A Global Assessment of the Resource Base for Direct Heat Utilization, *Renewable and Sustainable Energy Reviews*, **82**, (2018) 961–975.

McLean, K., and McNamara, D. D.: Fractures Interpreted from Acoustic Formation Imaging Technology: Correlation to Permeability, *Proceedings: 36th Workshop on Geothermal Reservoir Engineering, Stanford, USA*, (2011), 1-10.

McNamara, D. D., Lister, A., and Prior, D. J.: Calcite Sealing in a Fractured Geothermal Reservoir: Insights from Combined EBSD and Chemistry Mapping, *Journal of Volcanology and Geothermal Research*, **323**, (2016), 38–52.

Mitchell, T. M., and Faulkner, D. R.: Experimental Measurements of Permeability Evolution During Triaxial Compression of Initially Intact Crystalline Rocks and Implications for Fluid Flow in Fault Zones, *Journal of Geophysical Research: Solid Earth*, **113**(11), (2008), 1–16.

Olivares, V., Cembrano, J. M., Arancibia, G., Reyes, N., Herrera, V., and Faulkner, D. R.: Significado Tectonico y Migracion de Fluidos Hidrotermales en una Red de Fallas y Vetas de un Duplex de Rumbo: un Ejemplo del Sistema de Falla de Atacama, *Andean Geology*, **37**(2), (2010), 473–497.

Ortega, O. J., Marrett, R. A., and Laubach, S. E., A Scale-Independent Approach to Fracture Intensity and Average Spacing Measurement, *AAPG Bulletin*, **90**(2), (2006), 193–208.

Pérez-Flores, P., Veloso, E., Cembrano, J., Sánchez-Alfaro, P., Lizama, M., and Arancibia, G.:. Fracture Networks, Fluid Pathways and Paleostress at the Tolhuaca Geothermal Field, *Journal of Structural Geology*, **96**, (2017), 134–148.

Priest, S. D., Discontinuity Analysis for Rock Engineering**,** *Chapman & Hall, London, United Kingdom* (1993), pp.473.

Ramsay, J. G.: The Crack-Seal Mechanism of Rock Deformation, *Nature*, **284**, (1980), 135–139.

Robb, L.: Introduction to Ore-Forming Processes, Wiley-Blackwell, (2004), 384p.

Sanderson, D. J., and Nixon, C. W., The Use of Topology in Fracture Network Characterization**,** *Journal of Structural Geology*, **72**, (2015), 55-66.

Scheuber, E., and Andriessen, P. A. M.: The Kinematic and Geodynamic Significance of the Atacama Fault Zone, Northern Chile, *Journal of Structural Geology*, **12**(2), (1990), 243–257.

Scheuber, E., and González, G.: Tectonics of the Jurassic-Early Cretaceous Magmatic Arc of the north Chilean Coastal Cordillera (22°–26° S): A story of Crustal Deformation Along a Convergent Plate Boundary, *Tectonics*, **18**(5), (1999), 895–910.

Schulz, S. E., and Evans, J. P.: Mesoscopic Structure of the Punchbowl Fault, Southern California, and the Geologic and Geophysical Structure of Active Strike-Slip Faults, *Journal of Structural Geology*, **22**, (2000), 913-930.

Sibson, R. H.: Structural Permeability of Fluid-Driven Fault-Fracture Mesh, *Journal of Structural Geology*, **18**, (1996), 1031-1042.

Sibson, R. H.: Conditions for Fault-Valve Behavior, *Geological Society Special Publication*, **54**, (1990), 15–28.

Sibson, R. H.: A Brittle Failure Mode Plot Defining Conditions of High Flux Flow, *Economic Geology*, **95**, (2000), 41–48.

Simmons, S. F., and Christenson, B. W.: Origins of Calcite in a Boiling Geothermal System, *American Journal of Science*, **294**, (1994), 361–400.

Siratovich, P. A., von Aulock, F. W., Lavallée, Y., Cole, J. W., Kennedy, B. M., and Villeneuve, M. C.,: Thermoelastic Properties of the Rotokawa Andesite: A Geothermal Reservoir Constraint, *Journal of Volcanology and Geothermal Research*, **301**, (2015), 1-13.

Terzaghi, R., Sources of Error in Joint Surveys, *Geotechnique*, **15,** (1965), 287-297.

Wakabayashi, J., Hengesh, J. V, and Sawyer, T. L.: Four-dimensional Transform Fault Processes: Progressive Evolution of Step-Overs and Bends, *Tectonophysics*, **392**, (2004), 279–301.

Wallis, I. C., McNamara, D., Rowland, J. V., and Massiot, C.: The Nature of Fracture Permeability in the Basement Graywacke at Kawerau Geothermal Field, New Zealand, *37th Workshop on Geothermal Reservoir Engineering*, (2012), 1-9.

Wiltschko, D. V., and Morse, J. W.: Crystallization Pressure Versus "Crack Seal" as the Mechanism for Banded Veins, *Geology*, **29**, (2001), 79–82.

Woodcock, N. H., Dickson, J. A. D., and Tarasewicz, J. P. T.: Transient Permeability and Reseal Hardening in Fault Zones: Evidence from Dilation Breccia Textures, *Geological Society of London Special Publication*, **270**, (2007), 43–53.